Published in final edited form as:
Dev Biol. 2014 February 15; 386(2): 428–439. doi:10.1016/j.ydbio.2013.11.015.

Abnormal differentiation of dopaminergic neurons in zebrafish *trpm7* mutant larvae impairs development of the motor pattern

Amanda R. Decker[1,*], **Matthew S. McNeill**[2,*], **Aaron M. Lambert**[3], **Jeffrey D. Overton**[4], **Yu-Chia Chen**[5], **Ramón A. Lorca**[6], **Nicolas A. Johnson**[7], **Susan E. Brockerhoff**[7], **Durga P. Mohapatra**[6], **Heather MacArthur**[8], **Pertti Panula**[5], **Mark A. Masino**[3], **Loren W. Runnels**[4], and **Robert A. Cornell**[1,2,**]

[1]Department of Anatomy and Cell Biology, University of Iowa, Iowa City, IA 52242
[2]Interdisciplinary Graduate Program in Neuroscience, University of Iowa, Iowa City, IA 52242
[3]Department of Neuroscience, University of Minnesota, Minneapolis, MN 55455 [4]UMDNJ-Robert Wood Johnson Medical School, Piscataway, NJ 08854 [5]Neuroscience Center and Institute of Biomedicine/Anatomy, University of Helsinki, Finland [6]Department of Pharmacology, University of Iowa, Iowa City, IA 52245 [7]Department of Biochemistry, University of Washington, Seattle WA 98195 [8]Department of Pharmacological and Physiological Science, St. Louis University, St. Louis, MO 63104

Abstract

Transient receptor potential, melastatin-like 7 (Trpm7) is a combined ion channel and kinase implicated in the differentiation or function of many cell types. Early lethality in mice and frogs depleted of the corresponding gene impedes investigation of the functions of this protein particularly during later stages of development. By contrast, zebrafish *trpm7* mutant larvae undergo early morphogenesis normally and thus do not have this limitation. The mutant larvae are characterized by multiple defects including melanocyte cell death, transient paralysis, and an ion imbalance that leads to the development of kidney stones. Here we report a requirement for Trpm7 in differentiation or function of dopaminergic neurons in vivo. First, *trpm7* mutant larvae are hypomotile and fail to make a dopamine-dependent developmental transition in swim-bout length. Both of these deficits are partially rescued by the application of levodopa or dopamine. Second, histological analysis reveals that in *trpm7* mutants a significant fraction of dopaminergic neurons lack expression of tyrosine hydroxylase, the rate-limiting enzyme in dopamine synthesis. Third, *trpm7* mutants are unusually sensitive to the neurotoxin 1-methyl-4-phenylpyridinium, an oxidative stressor, and their motility is partially rescued by application of the iron chelator deferoxamine, an anti-oxidant. Finally, in SH-SY5Y cells, which model aspects of human dopaminergic neurons, forced expression of a channel-dead variant of TRPM7 causes cell death. In summary, a forward genetic screen in zebrafish has revealed that both melanocytes and

**Corresponding author: Robert A. Cornell, Associate Professor, Department of Anatomy and Cell Biology, 1-400D Bowen Science Building, Carver College of Medicine, The University of Iowa, Iowa City, Iowa 52242, Phone (319) 335-8908, FAX (319) 335-7198, robert-cornell@uiowa.edu.
*Equal contribution
Matthew McNeill's current address: Institute for Genomic Biology, 1206 W. Gregory, RM 2401G, University of Illinois, Urbana, IL.

Conflict of Interest: None

dopaminergic neurons depend on the ion channel Trpm7. The mechanistic underpinning of this dependence requires further investigation.

Keywords

Parkinson's; Zebrafish; Dopamine; TRPM7

Introduction

Transient receptor potential melastatin-like 7 (TRPM7), a widely-expressed divalent-cation channel with intrinsic kinase activity, has cell-type- and context-dependent roles in cell survival and physiology. Mouse and frog embryos depleted of the *Trpm7* gene die during early morphogenesis (Jin et al., 2008; Liu et al., 2011b; Ryazanova et al., 2010). Cell-lineage-specific deletion of *Trpm7* in mice indicates that Trpm7 is essential for the terminal differentiation of thymocytes and of certain neural-crest derivatives, including melanocytes and sensory neurons (Jin et al., 2008; Jin et al., 2012). Studies in cell lines or primary cells *in vitro* have suggested roles for TRPM7 in Mg^{2+} homeostasis (Chubanov et al., 2004; Nadler et al., 2001), cell proliferation (Hanano et al., 2004), cell adhesion (Su et al., 2006), and cholinergic synaptic transmission (Krapivinsky et al., 2006). The lack of TRPM7 causes cell-death due to a disruption of magnesium homeostasis in some cell lines (Kim et al., 2008; Nadler et al., 2001). Conversely, its presence appears to sensitize at least one cell type to zinc-ion poisoning (Inoue et al., 2010), and the reduction of *TRPM7* expression in fibroblasts decreased markers of oxidative stress and increased cellular resistance to apoptotic stimuli (Chen et al., 2012). Moreover, when extracellular levels of divalent cations drop below normal physiological levels TRPM7 permits an influx of Ca^{2+} which may contribute to excitotoxicity (Aarts et al., 2003; Sun et al., 2009; Wei et al., 2007). Supporting this model, reduction of *Trpm7* expression in the rat hippocampus was found to lessen the amount of neuronal cell death caused by ischemia (Sun et al., 2009). In summary, studies in cell lines and limited tissue specific knock-outs in rodents indicate that the physiological role for TRPM7 is cell-type dependent.

Additional roles for Trpm7 in vertebrate development were uncovered through forward genetics in zebrafish. Independent screens for mutations that disrupt melanophore development, early motility, or adult growth each identified *trpm7* mutants (Arduini and Henion, 2004; Cornell et al., 2004; Elizondo et al., 2005; Kelsh et al., 1996; Low et al., 2011). In *trpm7* loss-of-function mutants, embryonic melanophores (the melanin-producing cells of fish) succumb to cell death (Arduini and Henion, 2004; Cornell et al., 2004), and the melanosomes (the organelles that confine melanin) are structurally abnormal (McNeill et al., 2007). Because Trpm7 is required within melanophores (Arduini and Henion, 2004; Cornell et al., 2004), the melanophore cell-death in *trpm7* mutants may result from the release of toxic intermediates of melanin synthesis into the cytoplasm (Hochstein and Cohen, 1963; McNeill et al., 2007; Pawelek and Lerner, 1977). Additionally, *trpm7* mutant larvae are unresponsive to touch for a period of about 12 hrs during development (Arduini and Henion, 2004; Cornell et al., 2004; Kelsh et al., 1996; Low et al., 2011). This phenotype can be alleviated by forcing the expression of *trpm7* in primary sensory neurons, implying that Trpm7 is required transiently for function or differentiation of embryonic primary sensory neurons (Low et al., 2011). Finally, global homeostasis of divalent cations including calcium and magnesium is abnormal in *trpm7* mutant larvae leading to aberrant calcification of developing bones. This suggests a function for Trpm7 in the kidney-associated Corpuscle of Stannius where it is highly expressed (Elizondo et al., 2005; Elizondo et al., 2010). Consistent with conservation of Trpm7 function at least in some tissues, *trpm7* mutant larvae exhibit bradycardia as do mice with depletion of Trpm7 in cardiac myocytes (Arduini

and Henion, 2004; Sah et al., 2013). Analysis of zebrafish *trpm7* mutant larvae has complemented mammalian studies.

Here we report additional analyses of a zebrafish *trpm7* mutant and describe the consequences to a human dopaminergic cell-line of reducing TRPM7 activity. We identify behavioral and developmental defects in *trpm7* mutants that can be partially reversed by exogenous dopamine. Further we find abnormal gene expression, and increased sensitivity to a toxin, in dopaminergic neurons of such mutants. Dominant negative interference with TRPM7 causes death of the human dopaminergic cell line, suggesting a conserved role for TRPM7 in dopaminergic neurons. In summary, the result of a forward genetic screen in zebrafish has identified a previously unrecognized genetic requirement for Trpm7 in function and possibly survival of dopaminergic neurons.

Methods

Fish and embryo rearing

All standard animal protocols were approved by the Institutional Animal Care and Use Committee, and comply with USDA laws as well as PHS Guidelines. Zebrafish progeny and adults were reared under supervision of the University of Iowa Animal Care Unit, at 27.5°C on a normal illumination cycle (i.e., 14 hrs light, 10 hrs dark) unless otherwise noted. Embryos were generated and handled following standard methods (Westerfield, 1993), and staged by hours post fertilization (hpf) at 28.5°C (Kimmel et al., 1995). The highly penetrant *trpm7*^{b508} (Elizondo et al., 2005), and *mitfa*^{w2} (Lister et al., 1999) alleles were used for all experiments. Until the beginning of each experiment, all fish were raised in fish water (distilled water further purified by reverse osmosis and then supplemented with 0.30 g Crystal Sea® (Marinemix) (Marine Enterprises International; Baltimore, MD) per liter).

Motility assay

Motility was monitored using ZebraBox and Viewpoint software (version 3,10,0,42; Viewpoint Life Sciences, Inc.; Montreal, Quebec, Canada) under infrared light. Larvae were exposed to alternating cycles of light and dark, invisible to the camera, every 30 min as described (Emran et al., 2008); each light transition took approximately 1 msec. 96-well plates (Costar) were used for all experiments. At 4 days post fertilization (dpf), larvae were singly placed in wells with 300 μl of fish water. Larvae were placed into a 28.5°C incubator on a normal light cycle overnight. All experiments were completed in a quiet room at 5 dpf, between 10 AM and 2 PM. Larvae were allowed to acclimate in the Zebrabox measurement apparatus for 2 hrs before recording began. Larval locomotion was tracked with ViewPoint software. We defined motility as tracks moving less than 10 cm/sec but more than 0.1 cm/sec. Location and distance traveled were recorded and binned every 5 min as presented in Fig. 2.

Cultured melanocytes

30 hpf control embryos, defined as the wild-type and heterozygous mutant siblings of *trpm7* homozygous mutants, and *trpm7* homozygous mutant embryos (hereafter, *trpm7* mutants), identified by the strong reduction of cutaneous melanocytes, were transferred to calcium-free medium supplemented with 0.05% trypsin and 5 mM EDTA, crushed with a plastic pestle, incubated at 33°C, and gently triturated every 10 min for 30 min. Cultures were gently spun, the supernatant discarded, and the tissue pellet resuspended in cell medium. Cells were cultured overnight at 30°C, and electrophysiology carried out at room temperature (RT) the next morning. Cell medium, adapted from (Badakov and Jazwinska, 2006), is DMEM (Gibco, Invitrogen, Carlsbad, CA) supplemented with 15 % (v/v) fetal bovine serum (FBS; Atlanta Biologicals, Lawrenceville, GA), 100 units/ml penicillin

(Gibco), 100 mg/ml streptomycin (Gibco), 1 % (v/v) trout serum (Seagrow, product JJ80, East Coast Biologicals, North Berwick, ME), 20 ng/ml bovine insulin (Sigma, St. Louis, MO), 50 ng/ml basic fibroblast growth factor (Sigma), 62.5 μg/ml ampicillin, 25 ng/ml epidermal growth factor (Sigma), 1 % embryo extract. 100 % embryo extract consists of 200 embryos at 3 dpf rinsed in 0.5% bleach for 2 min then rinsed in calcium-free Ringer's solution (defined in (Westerfield, 1993)) for 2 min; the embryos were homogenized without liquid and suspended in 1 mL of cell medium without fetal bovine serum (FBS).

Cell Culture and Adenoviruses

The 293-TRPM7 cell line was employed to express hemagglutinin (HA)-tagged murine TRPM7 and has been previously described (Su et al., 2006). 293-TRPM7 cells were cultured in Dulbecco's Modified Eagle Medium (D-MEM) with 10 % FBS. The overexpression of HA-tagged TRPM7 in 293-TRPM7 cells was induced by the addition of tetracycline (1 μg/ml) to the growth medium for 24 hrs. To assess the dominant-negative potential of the TRPM7-E1047K pore mutant (TRPM7-DN), 293-TRPM7 cells were treated with tetracycline and transiently transfected with pcDNA5/FRT/TO-HA-TRPM7-E1047K, which has been previously described (Li et al., 2007). SH-SY5Y cells were maintained in D-MEM/F-12 with 10 % FBS and 5 % horse serum, and were differentiated in complete medium with 10 μM retinoic acid (RA), as previously described with the following modifications (Cheung et al., 2009). SH-SY5Y cells were placed in differentiation medium for 3 days prior to viral transduction. After the recombinant adenoviruses were applied at a multiplicity of infection (M.O.I.) of 30, cells were cultured in differentiation medium for another 3 days unless otherwise specified. Cell viability was quantified by manual cell counting and trypan blue exclusion. The recombinant adenoviruses expressing LacZ and GFP have been previously described (Su et al., 2011). The recombinant adenovirus expressing TRPM7-DN was engineered as follows. First, the AfeI/BglII fragment from pcDNA5/FRT/TO-HA-TRPM7-E1047K was exchanged with the AfeI/BgIII fragment from pENTR/D-TOPO-SR-TRPM7 to create pENTR/D-TOPO-SR-TRPM7-E1047K. The SR-TRPM7-E1047K cassette was then transferred to the destination vector pAd/CMV/V5-DEST (Invitrogen) by recombination using the Gateway® system (Invitrogen) following the manufacturer's instructions. The recombinant adenoviruses expressing SR-TRPM7-DN was then made using pAd/CMV/V5-SR-TRPM7-E1047K and the ViraPower Adenoviral Expression System (Invitrogen) following the manufacturer's instructions. The TRPM7-DN recombinant adenovirus was amplified and concentrated from two 150 mm plates of HEK-293A cells (Invitrogen) using the Adenopack 100 kit (Sartorius Stedim Biotech) following manufacturer's instructions.

Drug treatments

All drugs were purchased from Sigma-Aldrich (St. Louis, MO). Levodopa (L-dopa; 20 mM) was applied with ascorbic acid (100 μM) to delay oxidation of the former; ascorbic acid alone was applied in control experiments. L-dopa was applied in the morning at 5 dpf, and larvae were allowed to incubate for one hour before behavior recordings began. Dopamine (DA; 20 μM) was applied to both behavioral (free-swimming) and fictive preparations and had locomotor effects within 5 to 20 min, similar to the time course reported in previous studies (Lambert et al., 2012; Souza and Tropepe, 2011; Thirumalai and Cline, 2008). The effect of DA on episode duration was quantified during 20–30 min into the drug application. MPP^+ was applied at 500 μM. It was dissolved immediately prior to application at 50 hpf, and refreshed daily. Larvae were fixed for immunohistochemistry at 5 dpf. All drugs were diluted in fish water except in the case of peripheral nerve recordings (see below), in which drugs were diluted in extracellular recording solution.

Whole-cell voltage clamp recordings

The cells were kept under continuous perfusion of standard extracellular solution containing (in mM): 135 Na-Methanesulfonate (Na-$MeSO_3$), 5 CsCl, 1 $CaCl_2$ and 10 HEPES, pH 7.4 (adjusted with NaOH). 1 μM tetrodotoxin (TTX) was added to the extracellular buffer, in order to block voltage-gated Na^+ channel currents. Patch pipettes were pulled from borosilicate glass tubes (TW150F-4, World Precision Instruments, Sarasota, FL) and heat-polished at the tip to give a resistance of 3–5 mΩ when filled with the pipette solution containing (in mM): 120 Cs-$MeSO_3$, 5 CsCl, 2 $CaCl_2$, 10 EGTA and 10 HEPES, pH 7.2 (adjusted with CsOH). The free Ca^{2+} concentration in the pipette solution was calculated as 60 nM (MaxChelator, Stanford). All currents were recorded at room temperature using an Axopatch 200B patch-clamp amplifier (Molecular Devices, Sunnyvale, CA), low-pass filtered at 5 kHz and sampled at 10 kHz. All current acquisitions were made with the pClamp10 software (Molecular Devices, Sunnyvale, CA) and analyzed with Origin 7 software (OriginLab Corporation, Northampton, MA). The holding potential was −70 mV and the currents were recorded by applying a voltage-ramp from −120 mV to +100 mV for 500 ms. To determine the Trpm7 current component, recordings were performed from cells superfused with extracellular solution containing 10 mM NH_4Cl or 10 mM $MgCl_2$ for 2 min after the first set of recordings under standard extracellular conditions.

Whole-cell voltage clamp recordings of TRPM7 currents in 293-TRPM7 cells were elicited by voltage stimuli lasting 250 ms delivered every second using voltage ramps from −120 mV to +100 mV. Data were digitized at 2 kHz and digitally filtered at 1 kHz. The internal pipette solution for macroscopic current recordings contained (in mM) 145 Cs-methanesulfonate, 8 NaCl, 10 EGTA, and 10 4-(2-hydroxyethyl)-1-piperzineethanesulfonic acid (HEPES), pH adjusted to 7.2 with CsOH. The extracellular solution for whole-cell recordings contained (in mM) 140 NaCl, 5 KCl, 2 $CaCl_2$, 20 HEPES, and 10 glucose, pH adjusted to 7.4 with NaOH.

Peripheral nerve recordings

Fictive swimming was assessed via peripheral nerve recordings *in vivo* as described previously (Masino and Fetcho, 2005). Briefly, control and *trpm7* mutants were anesthetized with 0.02% Tricaine-S (Western Chemical) in extracellular recording solution (Lambert et al., 2012) and paralyzed with 0.1% (w/v) α-Bungarotoxin (Sigma). Larvae were pinned in a lateral position to a Sylgard-lined petri dish and the skin was removed. Subsequently, larvae were transferred to the stage of an Olympus BX51 WI microscope and extracellular recording solution was superfused continuously at 1 mL/min at room temperature. Extracellular suction electrode recording techniques (Masino and Fetcho, 2005) were used to monitor the activity of peripheral nerves during fictive behavior; the tip of the extracellular suction electrode (6–15 μm tip diameter) was positioned near the dorsoventral midline of an intermyotomal cleft where the skin had been removed. Spontaneous activity was acquired for a minimum of 30 min for each preparation and, for experiments in which DA was applied, samples were subsequently perfused with 20 μM DA in extracellular recording solution. All recordings were between body segments 10 and 20. A MultiClamp 700B (Molecular Devices, Sunnyvale, CA) amplifier was used to monitor extracellular voltage in current-clamp mode at a gain of 2,000 (Rf = 50 MOhm), with the low- and high-frequency cut-off at 300 and 1,000 Hz, respectively. Recordings were sampled at 10 kHz, digitized using a digitizing board (DigiData series 1440A, Molecular Devices, Sunnyvale, CA) and acquired using pClamp 10 software. Analysis of peripheral nerve activity was performed as described previously (Lambert et al., 2012; Wiggin et al., 2012), using custom scripts written in MATLAB (Mathworks, Natick MA). Briefly, the occurrence times of rhythmic fictive locomotor bursts were determined from a rectified and smoothed version of the voltage recording. These bursts were then grouped into episodes and used to determine

the episode durations for each voltage trace. Values for fictive episode durations are expressed as mean ± SEM (standard error of the mean).

Electroretinogram recordings

Electroretinograms (ERGs) were recorded as described previously (Lewis et al., 2011). Briefly, 6 dpf larvae were anesthetized in 0.02% Tricaine-S, and eyes were removed using a fine tungsten wire loop. Excised eyes were then placed in an oxygenated Ringer's solution (in mM; 130 NaCl, 2.5 KCl, 20 $NaHCO_3$, 0.7 $CaCl_2$, 1.0 $MgCl_2$, and 20 glucose), and a glass electrode was positioned directly onto the cornea. After 3 min of dark adaptation, eyes were exposed to white light flashes in the presence or absence of background light, and their electrical responses were recorded. Data were acquired and processed as described previously (Van Epps et al., 2001). Peak values are listed as the mean ± SD (standard deviation) from at least 3 animals.

Free-swimming assay

Video acquisition and analysis were performed as described previously (Lambert et al., 2012). Briefly, a group of ten larvae in embryo medium or embryo medium containing 20 μM DA was placed in a 50 mm watch glass (Fisher Scientific) atop a transmitted light stage (Schott TLS and MC-1500 LED Controller). The larvae were allowed to acclimate to the recording arena for 5 min prior to the start of video recording. Subsequently, spontaneous free-swimming was recorded for 10 min at 60 frames per second, using a digital CMOS camera (Point Grey, Firefly M) with an attached 50 mm macro lens (Sigma Corporation, Ronkonkoma, NY). Videos were acquired with Fview (open-source software; (Straw and Dickinson, 2009)), in uncompressed Fly Movie Format (FMF). The FMF files generated by Fview were imported into the California Institute of Technology Fly Tracker (Ctrax) (open-source software; (Branson et al., 2009)) to obtain independent trajectories of each target within the arena. We subsequently used the open-source Fix Errors MATLAB Toolbox, provided by the creators of Ctrax (Branson et al., 2009)), to identify and fix tracking errors (such as swapping of target identities). The total number of errors per 10-min video was 4.49 ± 0.55 (n = 23 videos) and all errors were corrected via the FEMT. Subsequently, scripts from the open-source Behavioral Microarray MATLAB Toolbox, provided by the creators of Ctrax (Branson et al., 2009), were implemented to compute descriptive statistics of a suite of behavioral parameters for each of the individual targets from the fixed Ctrax trajectories. The target speed function, velmag, was extracted for each target and custom scripts were written to define and detect swimming episodes using the same criteria as employed previously (Lambert et al., 2012), namely: signal threshold of 1.5 mm/sec, minimum episode duration of 66.6 ms (4 frames), minimum average swimming speed of 3 mm/sec, and concatenation of signals within a 300 ms (18 frame) inter-signal interval. Identical filters were applied for all videos across all ages and experimental groups. Once all swimming episodes were identified, we quantified the total distance traveled per individual in centimeters (sum of instantaneous speeds during swimming episodes divided by the frame rate) and mean swimming episode duration per individual in milliseconds (mean duration from the onset to the offset of each individual episode) over the 10-min recording period. Sample sizes were ultimately smaller for quantifying episode duration compared with total distance traveled because episode duration could not be obtained from animals that did not move during the recording session.

Histology

Larvae were fixed in 4% paraformaldehyde overnight at 4°C. Whole-mount larvae were washed out of fixative with double-distilled water (ddH_2O), permeabilized by either 5 hrs incubation at room temperature in ddH_2O or 30 min treatment with 40 mg/mL ProtK,

blocked in PBDT (Phosphate buffered solution, 2.5 % Goat serum, 1 % bovine serum albumin, 1 % DMSO, 0.5 % Tritonx-100) for 1 hr, and incubated in primary antibody [mouse anti-tyrosine hydroxylase (1:500, Sigma-Aldrich) or rabbit anti- 5HT] diluted in PBDT overnight at 4°C. In experiments where we used the peroxidase anti-peroxidase system (Jackson Immunoresearch Laboratories, West Grove, PA), we subsequently incubated embryos in 2° goat anti-mouse antibodies and 3° mPAP antibody. Samples were incubated in 1 % hydrogen peroxide for 30 min in between application of the 2° and 3° antibodies, and then developed using 3–3′-Diaminobenzidene (DAB, Sigma Aldrich). Whole-mount larvae were alternatively prepared using Alexa 488 conjugated secondary antibodies and optically sectioned using a Zeiss 700 confocal microscope and ZEN 2010 software (Carl Zeiss Inc., Germany). Optical sections were compressed into single images by projecting the maximum intensity signal of each pixel of each section using ImageJ (National Institutes of Health) for approximately 500 × 500 × 150 μm (width x height x depth) at a resolution of 1.087 pixels per μm. *In situ* hybridization for *th2* and *dat* were carried out as described (Sallinen et al., 2010).

Reverse transcriptase-polymerase chain reaction (RT-PCR)

Whole-animal mRNA was isolated at 5 dpf using Trizol (Invitrogen), from which cDNA was synthesized using oligo-dT(16) primers and the cDNA SuperScript cDNA synthesis kit (Qiagen). MMLV enzyme (Promega) was used for the reverse transcriptase reaction. Quantities of mRNA were calculated relative to levels of *beta-actin*. Primers for *beta-actin* forward 5′-gagatgatgcccctcgtg-3′ reverse 5′-gctcaatggggtatttgagg-3′; *th1* primers forward 5′-catatgtgacccgcatcaag-3′ reverse 5′-caacacattcagggcatctg-3′; *th2* primers forward 5′-agcttcgtgtttgaggagga-3′ reverse 5′-ctctttctgctcgctcgact-3′; *dat* primers forward 5′-agacatctgggaaggtggtg-3′ reverse 5′-tgtagctggagaaggcgatt-3′; *bdnf* primers forward 5′-tggcggcatccaggtagt-3′ reverse 5′-tcgaaggacgttgacctgtatg-3′.

Statistics

Levene's test for equality of variances was used to test assumptions about error variances for Student's t-test. For experiments that involved comparisons of two means, one-tailed Student's t-tests were performed when error variances were equal. Significance was determined at the $p < 0.05$ level. A Welch t-test was used instead when error variances were unequal. Multiple comparisons of means were made using two-way analysis of variance and Bonferroni post-hoc tests. SPSS Statistics (IBM version 19 was used for all above tests. A χ^2 test was conducted assuming Mendelian ratios of inheritance and 3 degrees of freedom, using Microsoft Excel.

Calcification Assays

Kidney stones were visualized as previously described (Elizondo et al., 2005). Briefly, live larvae were submerged in 0.004% alizarin red in Ringer's solution overnight. They were washed 2x in Ringer's solution before visualizing live under Texas Red filter.

Results

Sequence analysis of *trpm7* cDNA generated from *trpm7*^{b508} mutants indicated that the encoded TRPM7 protein is truncated in the cytoplasmic carboxy terminus upstream of the kinase domain; however it did not clarify whether this variant retains channel function (Elizondo et al., 2005). Application of a voltage ramp to melanocytes isolated from wild-type embryos at 48 hours post fertilization (hpf) produced currents characteristic of those mediated by TRPM7 (Fig. 1A). Subjecting rare surviving melanocytes isolated from 48 hpf *trpm7* mutants to the same procedure revealed that these produce virtually no such current (Fig. 1B). These findings suggest that, *in vivo*, *trpm7*^{b508} encodes a Trpm7 protein that

either lacks channel function or fails to reach the plasma membrane. They are consistent with conclusions derived from forced expression of *trpm7*^{b508} in Xenopus oocytes (Low et al., 2011).

Because an allele of *TRPM7* was reported to be associated with a parkinsonian condition (Hermosura et al., 2005), we observed motility in zebrafish *trpm7* mutant larvae at 5 days post fertilization (dpf). We monitored motility in larvae in alternating 30-minute periods of light and dark because the light-to-dark transition strongly stimulates swimming (Burgess and Granato, 2007; Emran et al., 2008). In dark periods and in light periods, *trpm7* homozygous mutants traveled a shorter distance than their siblings (wild-types and heterozygous mutants; hereafter, control larvae) (Fig. 2, statistical analysis in the figure legend). In both mutants and control larvae, motility was lower in light periods than in dark periods; in light periods mutants were virtually still. To test whether a deficit in dopaminergic signaling causes hypomotility in *trpm7* mutants, we treated *trpm7* mutants and control larvae with levodopa (L-dopa), a precursor of dopamine (DA), and assayed their motility. In dark periods, L-dopa-treated mutants moved significantly more than vehicle-treated mutants, while L-dopa treatment did not affect the motility of control larvae (Fig. 2). The effectiveness of the light-to-dark stimulus depends on intact visual processing and on non-visual light sensors (Emran et al., 2008; Fernandes et al., 2012). To test whether vision is grossly affected in *trpm7* mutants we subjected larvae to micro-electroretinography. We found that beta waves were indistinguishable between mutants and control larvae (Fig. S1). We conclude that hypomotility of the mutants is unlikely to be caused by abnormal vision or other gross defects. The simplest explanation of these observations is that hypomotility in *trpm7* larvae is at least partly the result of sub-threshold dopaminergic signaling in the central nervous system.

To test the possibility that dopaminergic signaling is lower than normal in *trpm7* mutants, we examined a developmental milestone in zebrafish that depends on intact dopaminergic signaling. Between 3 and 4 dpf, wild-type zebrafish larvae undergo a developmental switch in their locomotor pattern, transitioning from long to short swimming episodes (Buss and Drapeau, 2001; Lambert et al., 2012). The latter pattern persists into adulthood (Fuiman and Webb, 1988; Muller et al., 2000). This developmental switch is mediated by central dopaminergic signaling, which originates in the caudal diencephalon and acts in the spinal cord via the diencephalospinal tract (Lambert et al., 2012). Using videography, we measured swimming speed and episode duration before (3 dpf) (Fig. S2) and after (5–6 dpf) (Fig. 3 A, top) the developmental switch. In addition to these behavioral parameters, we measured the duration of fictive swimming episodes by carrying out extracellular recording of peripheral nerve activity (Fig. 3 A, bottom). At 3 dpf, there was no difference in episode duration between *trpm7* controls and mutants, regardless of whether examined in the behavioral or fictive swimming preparations (Fig. S2). However, at 5–6 dpf, the durations of behavioral and fictive episodes in *trpm7* mutants were significantly longer than those of controls (Fig. 3 A,B), indicating that the mutants did not properly execute the stereotypic switch from long to short episodes. By contrast, in 5–6 dpf *trpm7* mutants treated with 20 μM exogenous DA, the episode duration during both the behavioral and fictive assays was significantly shorter than in untreated *trpm7* mutants, but not different from that in controls (Fig. 3 A,B). Because the long-episode behavioral phenotype of *trpm7* mutants is recapitulated in the fictive swimming preparation, and because the exogenous application of DA is sufficient to rescue the developmentally appropriate locomotor pattern, we conclude that this phenotype is not caused by a deficit in muscle or body morphology but rather by to a lack of central dopaminergic signaling (Lambert et al., 2012).

We next used histology to determine if dopaminergic neurons and other neuronal sub-types are present in *trpm7* mutants. Tyrosine hydroxylase is the rate-limiting enzyme in dopamine

synthesis. There are two orthologs of *tyrosine hydroxylase* in zebrafish, Th1 and Th2 (Chen et al., 2009; Filippi et al., 2009; Holzschuh et al., 2001; Yamamoto et al., 2010). There is recent evidence that Th2 contributes to serotonin synthesis in larvae (Ren et al., 2013), although in some cells Th2 is detected together with DA in the absence of Th1, implying it contributes to dopamine synthesis (Yamamoto et al., 2011). Clusters of anti-Th1 immunoreactive (IR) cells (Th1 IR cells, hereafter) are present in several discrete clusters within the brains of 5-dpf zebrafish larvae (Fig. 4 M; the labeling scheme used here (Sallinen et al., 2009) is compared to an alternative scheme (Rink and Wullimann, 2002) in Table S1). The number of Th1 IR cells in all of these clusters appeared grossly reduced in mutants in comparison to controls. To quantify this effect, we focused on a cluster in the pretectum (group 7), which is well-separated from the other clusters, and on a cluster in the periventricular hypothalamus (group 13), because neurons here exhibit a high level of immunoreactivity and are less densely packed than elsewhere. We found that the number of Th1 IR cells in both clusters was significantly lower in *trpm7* mutants than in control larvae (Fig. 4 A–J). The number of cells expressing *th2*, which are found only in a preoptic cluster (group 3b), a diencephalic cluster (group 8b), and a posterior paraventricular organ cluster (group 10b), was also clearly reduced in *trpm7* mutants compared to controls (Fig. 4 K,L). The reduction in the number of *th1*- and *th2*-expressing cells was mirrored by a reduction of the total amount of *th1* and *th2* mRNA in mutants with respect to siblings, as monitored by qRT-PCR (Fig. 5 H). In contrast to expression of *th* paralogs, expression of *dopamine transporter* (*dat*), a second marker of dopaminergic neurons, appeared grossly equivalent in *trpm7* mutants and controls (Fig 5 E,F). Confirming this impression, we found the number of cells expressing GFP in the *Tg(dat:gfp)* transgenic line (Xi et al., 2011) was not significantly different in *trpm7* mutants relative to control larvae (Fig. 5 C,D). The number of sensory neurons in the dorsal root ganglia and the number of serotoninergic neurons in the pretectum, recognized by anti-Hu and anti-5-hydroxytryptophan (5HT) immunoreactivity, respectively, were equivalent in mutants and controls (Fig. 5 G and legend to Fig 5). We also found no difference between message levels of *brain derived neurotrophic factor (bdnf)*, a gene expressed in many regions of the brain (Fig. 5 H). These findings indicate that, in contrast to embryonic melanophores, which undergo cell death, dopaminergic neurons and other categories of neurons examined are present in normal numbers in *trpm7* mutants. However, abnormally low expression of *th* paralogs in such mutants indicates faulty differentiation or physiology of dopaminergic neurons and possibly a subset of serotoninergic neurons (i.e., those expressing Th2).

Embryonic melanophores in *trpm7* mutants are poisoned by the oxidative intermediates of melanin synthesis (McNeill et al., 2007), and such intermediates are related to dopamine; therefore we reasoned that dopaminergic neurons in *trpm7* mutants may similarly experience elevated levels of oxidative stress. In this case they may be hypersensitive to oxidative stressors. The neurotoxin 1-methyl-4-phenylpyridinium ion (MPP^+) is transported by the dopamine transporter into neurons, where it interferes with complex I of the mitochondrial electron transport chain, depleting the cell of ATP and elevating levels of reactive oxygen species (ROS) (reviewed in Segura Aguilar and Kostrzewa, 2004). We examined Th1 IR neurons in control and *trpm7* mutant larvae treated chronically with MPP^+. In control larvae, this treatment caused a 15 % reduction (relative to untreated larvae) in the number of Th1 IR cells in the pretectal area, whereas in *trpm7* mutants it caused a 50 % reduction (relative to untreated *trpm7* mutants) (Fig. 4 A-D, I). The increased sensitivity of *trpm7* mutants to the effects of MPP^+ was also apparent in the hypothalamus (Fig. 4 E-H, J). In principle, abnormally high levels of *dat* expression might explain the elevated sensitivity to MPP^+, but we found that the *dat* levels in mutants and siblings are comparable (as measured by qRT-PCR, Fig. 5 H). The increased sensitivity of *trpm7* mutants versus control larvae to MPP^+ implies that the absence of Trpm7 sensitizes DA neurons to oxidative stress.

We next asked whether treatments that protect DA neurons from MPP^+ may similarly protect them from the absence of Trpm7. Deferoxamine (DFO) chelates iron and thereby inhibits the iron-catalyzed conversion of hydrogen peroxide to the more highly reactive hydroxyl ion (Menasche et al., 1987). DFO protects against degeneration of dopaminergic neurons induced by 6-hydroxydopamine (6-OHDA) or MPTP (the MPP^+ precursor) in animal models (Ben-Shachar et al., 1992; Lan and Jiang, 1997). We treated *trpm7* mutants and controls chronically with DFO and measured their motility. Mutants treated with DFO moved significantly more than untreated mutants (Fig. 6), whereas control siblings were not affected by DFO treatment. DFO treatment did not have a detectable effect on the number of Th1 IR cells or on the quality of melanocytes in *trpm7* mutants (data not shown). Of note, treatment of *trpm7* mutant larvae with DFO, similar to their treatment with L-dopa, increased motility after the dark-to-light transition, but not after the light-to-dark transition. This suggests that DFO treatment partially rescues the function of dopaminergic neurons in *trpm7* mutants, and therefore that the defect in such neurons caused by the absence of Trpm7 is similar to that induced by 6-OHDA or MPTP treatment.

Because parkinsonian features can result from the calcification of basal ganglia (Koller et al., 1979), we considered the possibility that the effects of Trpm7 on dopaminergic neurons may be indirect. As previously reported (Elizondo et al., 2010), *trpm7* mutant embryos had significantly more kidney stones than controls. However we did not detect calcification in the brains of either genotype. We also found no correlation between average distance moved in the light-dark analysis and the presence of kidney stones (Pearson correlation coefficient of 0.015, n=43, two-tailed test of significance 0.51). These findings support the possibility that Trpm7 is required within dopaminergic neurons in zebrafish larvae, although this remains to be tested experimentally.

Because of distinct phenotypes in zebrafish and mouse *Trpm7* loss-of-function mutants, it is unknown whether there is requirement for TRPM7 within mammalian dopaminergic neurons. SH-SY5Y is a dopaminergic, neuroblastoma-derived cell line that can be induced to differentiate *in vitro* (Encinas et al., 2000). We infected SH-SY5Y cells with adenovirus encoding the TRPM7-E1047K channel-pore mutant form of TRPM7 (TRPM7-DN), or with a control adenovirus expressing LacZ. Electrophysiological recordings confirmed our expectation that TRPM7- E1047K acts in dominant-negative fashion, suppressing wild-type TRPM7 currents (Fig. 7 A,B). In comparison to non-transduced and LacZ-expressing SH-SY5Y cells, TRPM7-DN-expressing counterparts underwent cell death at an elevated rate, whether or not they were induced to differentiate (Fig. 7 C,D). Treatment with DFO did not alleviate the toxicity of TRPM7-DN (Fig. S3). These findings suggest that survival of a human dopaminergic cell-line requires Trpm7 in a cell-autonomous fashion.

Discussion

The zebrafish *trpm7* mutant provides an unusual opportunity to explore the roles for Trpm7 in cell differentiation and physiology at stages of development later than gastrulation, the stage when mice and frogs depleted of Trpm7 die. Here we have presented several pieces of evidence that in zebrafish *trpm7* loss-of-function mutants there is defective function of dopaminergic neurons leading to behavioral phenotypes. First, motility in *trpm7* mutant larvae in the dark can be elevated by a concentration of L-dopa that has no effect on sibling larvae. Tonic application of L-dopa probably poorly mimics endogenous dopamine (DA) signaling and may have indirect compensatory effects on Trpm7-dependent neuronal populations controlling motility. Nonetheless, these findings suggest that within *trpm7* mutants there is a defect in the production or release of DA while other elements of DA signaling relevant to motility remain intact. Second, the observation that *trpm7* mutants do not undergo the stereotypic, DA-dependent developmental switch from long to short

swimming episodes but will do so if provided with exogenous DA also suggests there lower-than-normal levels of dopaminergic signaling in *trpm7* mutants. It also implies that the signaling mechanisms and neural circuits that result in DA-mediated shortening of swimming episodes, which were previously shown to be separable from those that set motility levels (Lambert et al., 2012), function properly. Third, the numbers of expressing *th1*-expressing and *th2*-expressing neurons are modestly but significantly reduced in *trpm7* mutant larvae in comparison to sibling larvae. A concomitant reduction in DA production in the brain may account for motility defects in mutants. We conducted an HPLC analysis of biogenic amines in whole embryo lysates but, because of confounding effects of melanocytes, it was not sensitive enough to detect changes in levels of biogenic amines of the magnitude as changes in *th* expression (data not shown). A similar analysis of isolated brains may suffice to do so. Alternatively, the cause of lower-than-normal dopaminergic signaling in Trpm7 mutants may be other than reduced DA production; for instance there may be a defect in evacuation of DA from synaptic vesicles, as has been proposed in cholinergic vesicles (Brauchi et al., 2008; Krapivinsky et al., 2006). Because motility of *trpm7* mutants after a dark-to-light transition is not measurably restored by L-dopa treatment, there may be separate contributions of Trpm7 to motility other than its role in development or function of DA neurons. There is a recent report that Th2 has tryptophan hydroxylase activity (Ren et al., 2013). While the number of neurons that are immunoreactive for 5HT appears to be normal in Trpm7 mutant larvae, we cannot rule out a role for Trpm7 in function of serotonergic neurons. In summary, the physiological role of Trpm7 in motility of 5 dpf zebrafish larvae in dark periods is largely explained by a requirement in dopaminergic neurons, while its role in motility in the light phase remains unexplained.

The mechanistic underpinnings of the defect in the DA neurons in *trpm7* mutants remain unclear. However, two observations suggest that in DA neurons, as in melanocytes but in contrast to in other cell types (Chen et al., 2012), loss of Trpm7 elevates oxidative stress. First, *trpm7* mutants are unusually sensitive to treatment with MPP^+, a toxin that raises levels of reactive oxygen species and that prevents the differentiation of, and may kill, dopaminergic neurons in zebrafish (Burns et al., 1983; Heikkila et al., 1985; Sallinen et al., 2010). Second, mutants treated with DFO, an iron chelator and anti-oxidant that halts the Fenton reaction, were more motile than untreated animals. How might the loss of Trpm7 lead to increased oxidative stress in dopaminergic neurons *in vivo*? The primary defect may be a disruption of cellular magnesium homeostasis, as organismal magnesium levels are abnormal in zebrafish *trpm7* mutants (Elizondo et al., 2010), and there is some evidence connecting abnormal cellular magnesium homeostasis and risk for Parkinson's disease (see references in Kolisek et al., 2013). In zebrafish *trpm7* mutants, melanocytes have abnormally shaped melanosomes and undergo cell death that is rescued by inhibition of tyrosinase (McNeill et al., 2007). Perhaps in the absence of Trpm7 the integrity of dopaminergic vesicles is also compromised, and the toxic molecule dopamine is released into the cytoplasm. How Trpm7 affects the integrity of these vesicles is unknown, but it is noteworthy that calcium channel blockers can cause a loss of the ATP-dependent proton gradient in catecholaminergic vesicles, reduce DA content, and can promote cell death among dopaminergic neurons (Terland and Flatmark, 1999). In summary, in the absence of Trpm7, defective cation homeostasis leading to elevated oxidative stress plausibly disrupts function, differentiation, and survival of dopaminergic neurons, but at present this model is speculative.

While there is no clear link between TRPM7 and any human disorder, the mechanisms by which DA neurons are compromised in the zebrafish *trpm7* mutants may be relevant to clinical conditions. Amyotrophic lateral sclerosis/parkinsonian dementia complex (ALS/PDC) is a disease to which epidemiologists have long ascribed an environmental cause

(Banack and Cox, 2003). A variant of TRPM7 with increased sensitivity to inhibition by magnesium was found to be over-represented in families with ALS/PDC in Guam (Hermosura et al., 2005) but not in the Kii peninsula of Japan (Hara et al., 2010). Evidence of a role for this ion channel in function and maintenance of dopaminergic neurons presented here supports further investigation into the possibility that mutations in *TRPM7* predispose individuals to ALS/PDC. Indeed, zebrafish *trpm7* mutants may serve as a model for the gene-environment interaction underlying ALS/PDC. Also, there is an association between risks for Parkinson's disease and metastatic melanoma (Liu et al., 2011a; Pan et al., 2011). This association has been proposed to result from failure of a mechanism used to contain quinone-related toxins in both dopaminergic neurons and melanocytes (Hernandez, 2009); TRPM7 may contribute to such a mechanism. Finally, stem cell-based therapies have the potential to restore the damage caused by neurodegenerative diseases. Such therapies require a clear understanding of the mechanisms that govern the differentiation and survival of dopaminergic neurons, including the role of TRPM7 in these processes (Hegarty et al., 2013).

Supplementary Material

Refer to Web version on PubMed Central for supplementary material.

Acknowledgments

We are grateful to Austin Keeler, Hayley Martin, Christine Roenitz, Melina Hale, and Jonathan Doorn for preliminary work on this project. We thank James Gambrell for statistical consultation and Alan Kay for useful discussions and for chelators. This work was supported by NIH grants NIEHS/NIH P30 ES05605 (University of Iowa Environmental Health Sciences Research Center), GM067841 (RAC), R01EY018814 (SEB), R01EY015165 (SEB), Core Grant P30EY001730 (UW), NS069898 (DPM), NS065054 (MAM), RO1GM080753 (LWR), Academy of Finland 116177 (PP), Sigrid Juselius Foundation (PP).

References

Aarts M, Iihara K, Wei WL, Xiong ZG, Arundine M, Cerwinski W, MacDonald JF, Tymianski M. A key role for TRPM7 channels in anoxic neuronal death. Cell. 2003; 115:863–877. [PubMed: 14697204]

Arduini BL, Henion PD. Melanophore sublineage-specific requirement for zebrafish touchtone during neural crest development. Mech Dev. 2004; 121:1353–1364. [PubMed: 15454265]

Badakov R, Jazwinska A. Efficient transfection of primary zebrafish fibroblasts by nucleofection. Cytotechnology. 2006; 51:105–110. [PubMed: 19002901]

Banack SA, Cox PA. Biomagnification of cycad neurotoxins in flying foxes: implications for ALS-PDC in Guam. Neurology. 2003; 61:387–389. [PubMed: 12913204]

Ben-Shachar D, Eshel G, Riederer P, Youdim MB. Role of iron and iron chelation in dopaminergic-induced neurodegeneration: implication for Parkinson's disease. Annals of neurology. 1992; 32(Suppl):S105–110. [PubMed: 1510367]

Branson K, Robie AA, Bender J, Perona P, Dickinson MH. High-throughput ethomics in large groups of Drosophila. Nat Methods. 2009; 6:451–457. [PubMed: 19412169]

Brauchi S, Krapivinsky G, Krapivinsky L, Clapham DE. TRPM7 facilitates cholinergic vesicle fusion with the plasma membrane. Proceedings of the National Academy of Sciences of the United States of America. 2008; 105:8304–8308. [PubMed: 18539771]

Burgess HA, Granato M. Modulation of locomotor activity in larval zebrafish during light adaptation. The Journal of experimental biology. 2007; 210:2526–2539. [PubMed: 17601957]

Burns RS, Chiueh CC, Markey SP, Ebert MH, Jacobowitz DM, Kopin IJ. A primate model of parkinsonism: selective destruction of dopaminergic neurons in the pars compacta of the substantia nigra by N-methyl-4-phenyl-1,2,3,6-tetrahydropyridine. Proceedings of the National Academy of Sciences of the United States of America. 1983; 80:4546–4550. [PubMed: 6192438]

Buss RR, Drapeau P. Synaptic drive to motoneurons during fictive swimming in the developing zebrafish. J Neurophysiol. 2001; 86:197–210. [PubMed: 11431502]

Chen HC, Su LT, Gonzalez-Pagan O, Overton JD, Runnels LW. A key role for Mg(2+) in TRPM7's control of ROS levels during cell stress. Biochem J. 2012; 445:441–448. [PubMed: 22587440]

Chen YC, Priyadarshini M, Panula P. Complementary developmental expression of the two tyrosine hydroxylase transcripts in zebrafish. Histochem Cell Biol. 2009; 132:375–381. [PubMed: 19603179]

Cheung YT, Lau WK, Yu MS, Lai CS, Yeung SC, So KF, Chang RC. Effects of all-trans-retinoic acid on human SH-SY5Y neuroblastoma as in vitro model in neurotoxicity research. Neurotoxicology. 2009; 30:127–135. [PubMed: 19056420]

Chubanov V, Waldegger S, Mederos y Schnitzler M, Vitzthum H, Sassen MC, Seyberth HW, Konrad M, Gudermann T. Disruption of TRPM6/TRPM7 complex formation by a mutation in the TRPM6 gene causes hypomagnesemia with secondary hypocalcemia. Proceedings of the National Academy of Sciences of the United States of America. 2004; 101:2894–2899. [PubMed: 14976260]

Cornell RA, Yemm E, Bonde G, Li W, d'Alencon C, Wegman L, Eisen J, Zahs A. Touchtone promotes survival of embryonic melanophores in zebrafish. Mech Dev. 2004; 121:1365–1376. [PubMed: 15454266]

Elizondo MR, Arduini BL, Paulsen J, MacDonald EL, Sabel JL, Henion PD, Cornell RA, Parichy DM. Defective skeletogenesis with kidney stone formation in dwarf zebrafish mutant for trpm7. Curr Biol. 2005; 15:667–671. [PubMed: 15823540]

Elizondo MR, Budi EH, Parichy DM. trpm7 regulation of in vivo cation homeostasis and kidney function involves stanniocalcin 1 and fgf23. Endocrinology. 2010; 151:5700–5709. [PubMed: 20881241]

Emran F, Rihel J, Dowling JE. A behavioral assay to measure responsiveness of zebrafish to changes in light intensities. J Vis Exp. 2008

Encinas M, Iglesias M, Liu Y, Wang H, Muhaisen A, Cena V, Gallego C, Comella JX. Sequential treatment of SH-SY5Y cells with retinoic acid and brain-derived neurotrophic factor gives rise to fully differentiated, neurotrophic factor-dependent, human neuron-like cells. Journal of neurochemistry. 2000; 75:991–1003. [PubMed: 10936180]

Fernandes AM, Fero K, Arrenberg AB, Bergeron SA, Driever W, Burgess HA. Deep brain photoreceptors control light-seeking behavior in zebrafish larvae. Current biology: CB. 2012; 22:2042–2047. [PubMed: 23000151]

Filippi A, Mahler J, Schweitzer J, Driever W. Expression of the paralogous tyrosine hydroxylase encoding genes th1 and th2 reveals the full complement of dopaminergic and noradrenergic neurons in zebrafish larval and juvenile brain. J Comp Neurol. 2009; 518:423–438. [PubMed: 20017209]

Fuiman LA, Webb PW. Ontogeny of Routine Swimming Activity and Performance in Zebra Danios (Teleostei, Cyprinidae). Anim Behav. 1988; 36:250–261.

Hanano T, Hara Y, Shi J, Morita H, Umebayashi C, Mori E, Sumimoto H, Ito Y, Mori Y, Inoue R. Involvement of TRPM7 in cell growth as a spontaneously activated Ca2+ entry pathway in human retinoblastoma cells. J Pharmacol Sci. 2004; 95:403–419. [PubMed: 15286426]

Hara K, Kokubo Y, Ishiura H, Fukuda Y, Miyashita A, Kuwano R, Sasaki R, Goto J, Nishizawa M, Kuzuhara S, Tsuji S. TRPM7 is not associated with amyotrophic lateral sclerosis-parkinsonism dementia complex in the Kii peninsula of Japan. American journal of medical genetics. Part B, Neuropsychiatric genetics: the official publication of the International Society of Psychiatric. Genetics. 2010; 153B:310–313.

Hegarty SV, Sullivan AM, O'Keeffe GW. Midbrain dopaminergic neurons: A review of the molecular circuitry that regulates their development. Developmental biology. 2013

Heikkila RE, Nicklas WJ, Vyas I, Duvoisin RC. Dopaminergic toxicity of rotenone and the 1-methyl-4-phenylpyridinium ion after their stereotaxic administration to rats: implication for the mechanism of 1-methyl-4-phenyl-1,2,3,6-tetrahydropyridine toxicity. Neuroscience letters. 1985; 62:389–394. [PubMed: 3912685]

Hermosura MC, Nayakanti H, Dorovkov MV, Calderon FR, Ryazanov AG, Haymer DS, Garruto RM. A TRPM7 variant shows altered sensitivity to magnesium that may contribute to the pathogenesis of two Guamanian neurodegenerative disorders. Proceedings of the National Academy of Sciences of the United States of America. 2005; 102:11510–11515. [PubMed: 16051700]

Hernandez EH. Pigmentation genes link Parkinson's disease to melanoma, opening a window on both etiologies. Med Hypotheses. 2009; 72:280–284. [PubMed: 19027242]

Hochstein P, Cohen G. The cytotoxicity of melanin precursors. Annals of the New York Academy of Sciences. 1963; 100:876–886. [PubMed: 13963743]

Holzschuh J, Ryu S, Aberger F, Driever W. Dopamine transporter expression distinguishes dopaminergic neurons from other catecholaminergic neurons in the developing zebrafish embryo. Mech Dev. 2001; 101:237–243. [PubMed: 11231083]

Inoue K, Branigan D, Xiong ZG. Zinc-induced Neurotoxicity Mediated by Transient Receptor Potential Melastatin 7 Channels. The Journal of biological chemistry. 2010; 285:7430–7439. [PubMed: 20048154]

Jin J, Desai BN, Navarro B, Donovan A, Andrews NC, Clapham DE. Deletion of Trpm7 disrupts embryonic development and thymopoiesis without altering Mg2+ homeostasis. Science. 2008; 322:756–760. [PubMed: 18974357]

Jin J, Wu LJ, Jun J, Cheng X, Xu H, Andrews NC, Clapham DE. The channel kinase, TRPM7, is required for early embryonic development. Proceedings of the National Academy of Sciences of the United States of America. 2012; 109:E225–233. [PubMed: 22203997]

Kelsh RN, Brand M, Jiang YJ, Heisenberg CP, Lin S, Haffter P, Odenthal J, Mullins MC, van Eeden FJ, Furutani-Seiki M, Granato M, Hammerschmidt M, Kane DA, Warga RM, Beuchle D, Vogelsang L, Nusslein-Volhard C. Zebrafish pigmentation mutations and the processes of neural crest development. Development. 1996; 123:369–389. [PubMed: 9007256]

Kim BJ, Park EJ, Lee JH, Jeon JH, Kim SJ, So I. Suppression of transient receptor potential melastatin 7 channel induces cell death in gastric cancer. Cancer Sci. 2008; 99:2502–2509. [PubMed: 19032368]

Kimmel CB, Ballard WW, Kimmel SR, Ullmann B, Schilling TF. Stages of embryonic development of the zebrafish. Dev Dyn. 1995; 203:253–310. [PubMed: 8589427]

Kolisek M, Sponder G, Mastrototaro L, Smorodchenko A, Launay P, Vormann J, Schweigel-Rontgen M. Substitution p.A350V in Na(+)/Mg(2)(+) exchanger SLC41A1, potentially associated with Parkinson's disease, is a gain-of-function mutation. PloS one. 2013; 8:e71096. [PubMed: 23976986]

Koller WC, Cochran JW, Klawans HL. Calcification of the basal ganglia: computerized tomography and clinical correlation. Neurology. 1979; 29:328–333. [PubMed: 571978]

Krapivinsky G, Mochida S, Krapivinsky L, Cibulsky SM, Clapham DE. The TRPM7 ion channel functions in cholinergic synaptic vesicles and affects transmitter release. Neuron. 2006; 52:485–496. [PubMed: 17088214]

Lambert AM, Bonkowsky JL, Masino MA. The conserved dopaminergic diencephalospinal tract mediates vertebrate locomotor development in zebrafish larvae. The Journal of neuroscience: the official journal of the Society for Neuroscience. 2012; 32:13488–13500. [PubMed: 23015438]

Lan J, Jiang DH. Desferrioxamine and vitamin E protect against iron and MPTP-induced neurodegeneration in mice. J Neural Transm. 1997; 104:469–481. [PubMed: 9295179]

Lewis A, Wilson N, Stearns G, Johnson N, Nelson R, Brockerhoff SE. Celsr3 is required for normal development of GABA circuits in the inner retina. PLoS genetics. 2011; 7:e1002239. [PubMed: 21852962]

Li M, Du J, Jiang J, Ratzan W, Su LT, Runnels LW, Yue L. Molecular determinants of Mg2+ and Ca2+ permeability and pH sensitivity in TRPM6 and TRPM7. The Journal of biological chemistry. 2007; 282:25817–25830. [PubMed: 17599911]

Lister JA, Robertson CP, Lepage T, Johnson SL, Raible DW. nacre encodes a zebrafish microphthalmia-related protein that regulates neural-crest-derived pigment cell fate. Development. 1999; 126:3757–3767. [PubMed: 10433906]

Liu R, Gao X, Lu Y, Chen HL. Meta-analysis of the relationship between Parkinson disease and melanoma. Neurology. 2011a; 76:2002–2009. [PubMed: 21646627]

Liu W, Su LT, Khadka DK, Mezzacappa C, Komiya Y, Sato A, Habas R, Runnels LW. TRPM7 regulates gastrulation during vertebrate embryogenesis. Developmental biology. 2011b; 350:348–357. [PubMed: 21145885]

Low SE, Amburgey K, Horstick E, Linsley J, Sprague SM, Cui WW, Zhou W, Hirata H, Saint-Amant L, Hume RI, Kuwada JY. TRPM7 is required within zebrafish sensory neurons for the activation of touch-evoked escape behaviors. The Journal of neuroscience: the official journal of the Society for Neuroscience. 2011; 31:11633–11644. [PubMed: 21832193]

Masino MA, Fetcho JR. Fictive swimming motor patterns in wild type and mutant larval zebrafish. J Neurophysiol. 2005; 93:3177–3188. [PubMed: 15673549]

McNeill MS, Paulsen J, Bonde G, Burnight E, Hsu MY, Cornell RA. Cell death of melanophores in zebrafish trpm7 mutant embryos depends on melanin synthesis. J Invest Dermatol. 2007; 127:2020–2030. [PubMed: 17290233]

Menasche P, Grousset C, Gauduel Y, Mouas C, Piwnica A. Prevention of hydroxyl radical formation: a critical concept for improving cardioplegia. Protective effects of deferoxamine. Circulation. 1987; 76:V180–185. [PubMed: 2822288]

Muller UK, Stamhuis EJ, Videler JJ. Hydrodynamics of unsteady fish swimming and the effects of body size: comparing the flow fields of fish larvae and adults. The Journal of experimental biology. 2000; 203:193–206. [PubMed: 10607529]

Nadler MJ, Hermosura MC, Inabe K, Perraud AL, Zhu Q, Stokes AJ, Kurosaki T, Kinet JP, Penner R, Scharenberg AM, Fleig A. LTRPC7 is a Mg.ATP-regulated divalent cation channel required for cell viability. Nature. 2001; 411:590–595. [PubMed: 11385574]

Pan TH, Li XQ, Jankovic J. The association between Parkinson's disease and melanoma. Int J Cancer. 2011; 128:2251–2260. [PubMed: 21207412]

Pawelek JM, Lerner AB. Cytotoxicity of Melanin Precursors. Yale J Biol Med. 1977; 50:576–576.

Ren G, Li S, Zhong H, Lin S. Zebrafish tyrosine hydroxylase 2 gene encodes tryptophan hydroxylase. The Journal of biological chemistry. 2013; 288:22451–22459. [PubMed: 23754283]

Rink E, Wullimann MF. Connections of the ventral telencephalon and tyrosine hydroxylase distribution in the zebrafish brain (Danio rerio) lead to identification of an ascending dopaminergic system in a teleost. Brain Res Bull. 2002; 57:385–387. [PubMed: 11922994]

Ryazanova LV, Rondon LJ, Zierler S, Hu Z, Galli J, Yamaguchi TP, Mazur A, Fleig A, Ryazanov AG. TRPM7 is essential for Mg(2+) homeostasis in mammals. Nature communications. 2010; 1:109.

Sah R, Mesirca P, Van den Boogert M, Rosen J, Mably J, Mangoni ME, Clapham DE. Ion channel-kinase TRPM7 is required for maintaining cardiac automaticity. Proceedings of the National Academy of Sciences of the United States of America. 2013; 110:E3037–3046. [PubMed: 23878236]

Sallinen V, Kolehmainen J, Priyadarshini M, Toleikyte G, Chen YC, Panula P. Dopaminergic cell damage and vulnerability to MPTP in Pink1 knockdown zebrafish. Neurobiology of disease. 2010; 40:93–101. [PubMed: 20600915]

Sallinen V, Torkko V, Sundvik M, Reenila I, Khrustalyov D, Kaslin J, Panula P. MPTP and MPP+ target specific aminergic cell populations in larval zebrafish. J Neurochem. 2009; 108:719–731. [PubMed: 19046410]

Segura Aguilar J, Kostrzewa RM. Neurotoxins and neurotoxic species implicated in neurodegeneration. Neurotox Res. 2004; 6:615–630. [PubMed: 15639792]

Souza BR, Tropepe V. The role of dopaminergic signalling during larval zebrafish brain development: a tool for investigating the developmental basis of neuropsychiatric disorders. Reviews in the neurosciences. 2011; 22:107–119. [PubMed: 21615265]

Straw AD, Dickinson MH. Motmot, an open-source toolkit for realtime video acquisition and analysis. Source Code Biol Med. 2009; 4:5. [PubMed: 19624853]

Su LT, Agapito MA, Li M, Simonson WT, Huttenlocher A, Habas R, Yue L, Runnels LW. TRPM7 regulates cell adhesion by controlling the calcium-dependent protease calpain. The Journal of biological chemistry. 2006; 281:11260–11270. [PubMed: 16436382]

Su LT, Liu W, Chen HC, Gonzalez-Pagan O, Habas R, Runnels LW. TRPM7 regulates polarized cell movements. Biochem J. 2011; 434:513–521. [PubMed: 21208190]

Sun HS, Jackson MF, Martin LJ, Jansen K, Teves L, Cui H, Kiyonaka S, Mori Y, Jones M, Forder JP, Golde TE, Orser BA, Macdonald JF, Tymianski M. Suppression of hippocampal TRPM7 protein prevents delayed neuronal death in brain ischemia. Nat Neurosci. 2009; 12:1300–1307. [PubMed: 19734892]

Terland O, Flatmark T. Drug-induced parkinsonism: cinnarizine and flunarizine are potent uncouplers of the vacuolar H+-ATPase in catecholamine storage vesicles. Neuropharmacology. 1999; 38:879–882. [PubMed: 10465691]

Thirumalai V, Cline HT. Endogenous dopamine suppresses initiation of swimming in prefeeding zebrafish larvae. J Neurophysiol. 2008; 100:1635–1648. [PubMed: 18562547]

Van Epps HA, Yim CM, Hurley JB, Brockerhoff SE. Investigations of photoreceptor synaptic transmission and light adaptation in the zebrafish visual mutant nrc. Investigative ophthalmology & visual science. 2001; 42:868–874. [PubMed: 11222552]

Wei WL, Sun HS, Olah ME, Sun X, Czerwinska E, Czerwinski W, Mori Y, Orser BA, Xiong ZG, Jackson MF, Tymianski M, MacDonald JF. TRPM7 channels in hippocampal neurons detect levels of extracellular divalent cations. Proceedings of the National Academy of Sciences of the United States of America. 2007; 104:16323–16328. [PubMed: 17913893]

Westerfield, M. The Zebrafish Book. University of Oregon Press; Eugene, OR: 1993.

Wiggin TD, Anderson TM, Eian J, Peck JH, Masino MA. Episodic swimming in the larval zebrafish is generated by a spatially distributed spinal network with modular functional organization. J Neurophysiol. 2012; 108:925–934. [PubMed: 22572943]

Xi Y, Yu M, Godoy R, Hatch G, Poitras L, Ekker M. Transgenic zebrafish expressing green fluorescent protein in dopaminergic neurons of the ventral diencephalon. Dev Dyn. 2011; 240:2539–2547. [PubMed: 21932324]

Yamamoto K, Ruuskanen JO, Wullimann MF, Vernier P. Two tyrosine hydroxylase genes in vertebrates New dopaminergic territories revealed in the zebrafish brain. Molecular and cellular neurosciences. 2010; 43:394–402. [PubMed: 20123022]

Yamamoto K, Ruuskanen JO, Wullimann MF, Vernier P. Differential expression of dopaminergic cell markers in the adult zebrafish forebrain. J Comp Neurol. 2011; 519:576–598. [PubMed: 21192085]

Highlights

- Zebrafish *trpm7* mutant larvae exhibit dopamine-responsive behavioral deficits.
- In such larvae, dopaminergic neurons express DAT but many lack expression of TH.
- *trpm7* mutant larvae are hyper-sensitive to a toxin of dopaminergic neurons, MPTP.
- We show that SH-SY5Y cells, which are dopaminergic, depend on TRPM7 for survival.
- How Trpm7 contributes to function and viability of dopaminergic neurons is unknown.

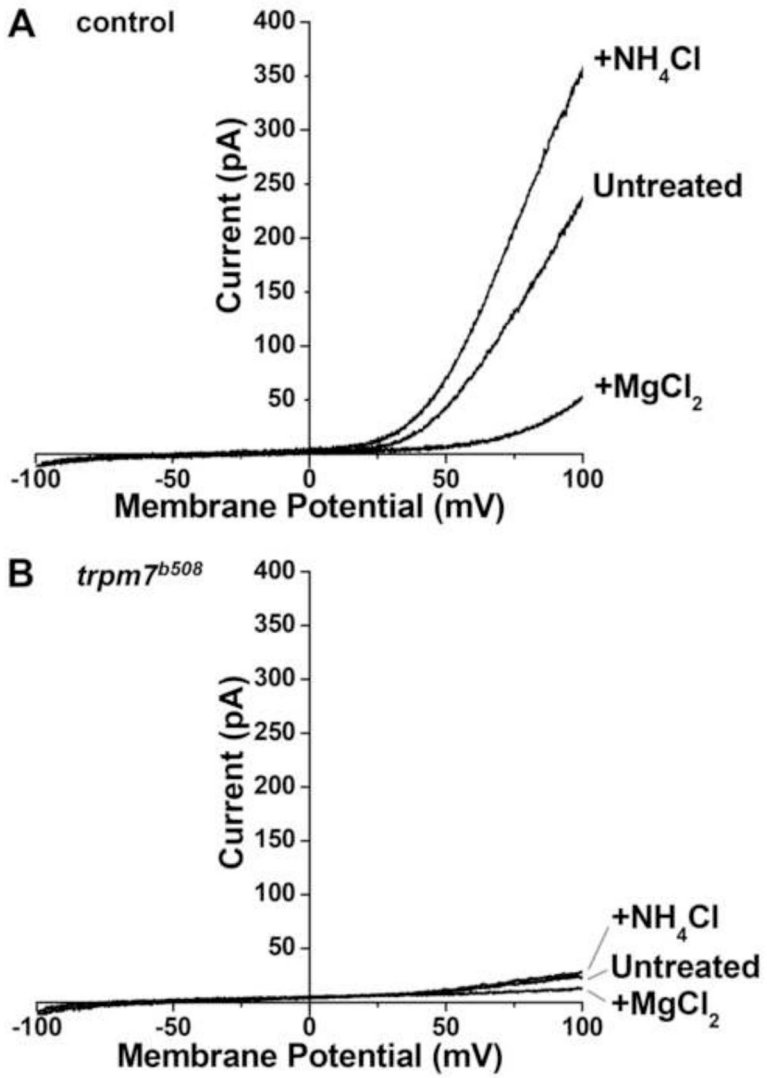

Figure 1. The TRPM7-like current is dramatically reduced in *trpm7*^{b508} mutants

Representative whole-cell current recordings of melanophores isolated at 32 hpf, in **A)** control or **B)** *trpm7* mutant embryos, in response to voltage ramps from −100 mV to +100 mV for 500 ms. **A)** Control melanocytes exhibited outwardly rectifying currents that are potentiated by the extracellular application of 10 mM NH_4Cl, and inhibited by the application of 10 mM $MgCl_2$, properties that are characteristic of TRPM7-mediated currents. **B)** The mutant melanophores did not exhibit any TRPM7-like outwardly rectifying currents. The slight outward rectification of currents in mutant melanophores indicates that the cells were alive. Control, n=7 cells; mutant, n=3 cells.

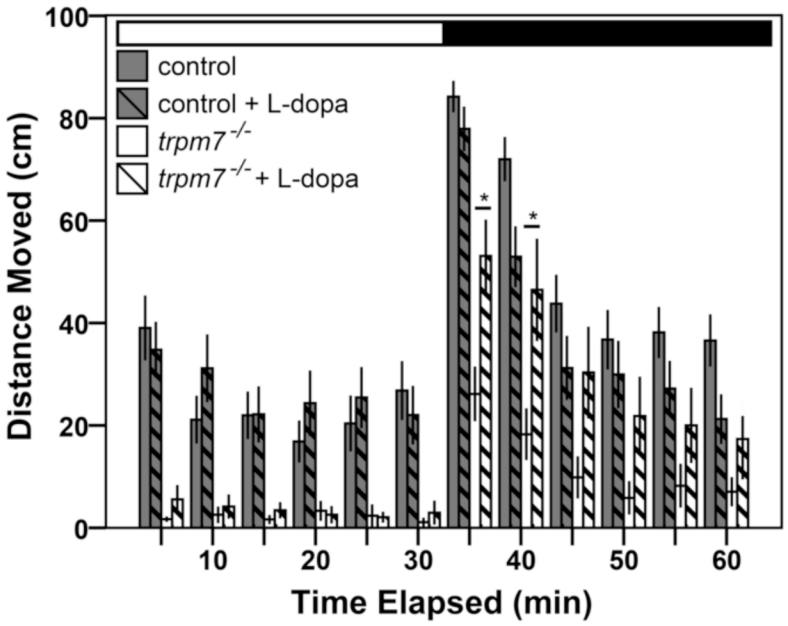

Figure 2. The hypomotility of *trpm7* mutants is levodopa responsive

Bar chart showing results of automated analysis of motility was carried out during daytime, over one cycle of 30 min exposure to light (white horizontal bar) followed by 30 min of darkness (black horizontal bar). Vertical bars indicate average distance moved during 5 min intervals. The average movement of mutants over the hour was significantly lower than that of controls (Welch t-test, $p < 0.001$). For each experiment, half of a single clutch of larvae from *trpm7* heterozygous adults was treated with 30 μM L-dopa for 3 hrs before recording. The motility of *trpm7* mutants was significantly increased by L-dopa treatment during the first 10 min after the light-to-dark shift (Student's t-test, $p = 0.004$ and Welch t-test, $p = 0.017$ for the first and second 5 min intervals after the light-to-dark transition, respectively). By contrast, control larvae were unaffected by L-dopa (Student's t-test, $p = 0.097$ and $p = 0.070$ for the first and second 5 min intervals after the light-to-dark transition, respectively). Each group tested consisted of 22–24 animals. Error bars represent SEM in one single hr. Asterisks, values significantly different.

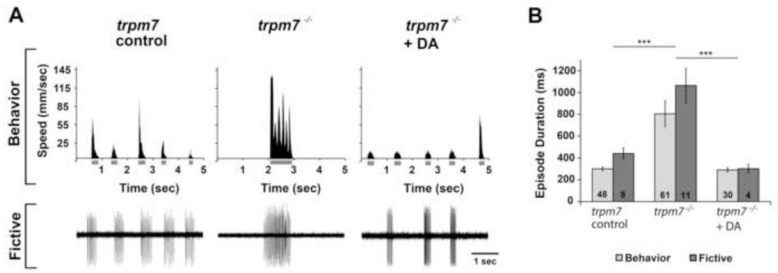

Figure 3. Dopamine rescues behavioral and fictive locomotor patterns of the *trpm7* mutant

A) (Top row) Representative recordings of speed and (bottom row) extracellular peripheral nerve recordings in fictive swimming preparations for discrete swimming episodes of 5–6 dpf control siblings (left), *trpm7* mutants (middle), and *trpm7* mutants + DA (20 μM; right). Grey bars below x-axes of speed plots represent episode durations whose beginnings and ends are defined by the filter settings. **B)** Summary plot of the mean durations of behavioral and fictive swimming episodes for each group. Asterisks indicate significant difference; *** $p < 0.001$. Numbers at the base of bars in graph denote number of larvae observed for each experimental group. Error bars represent SEM.

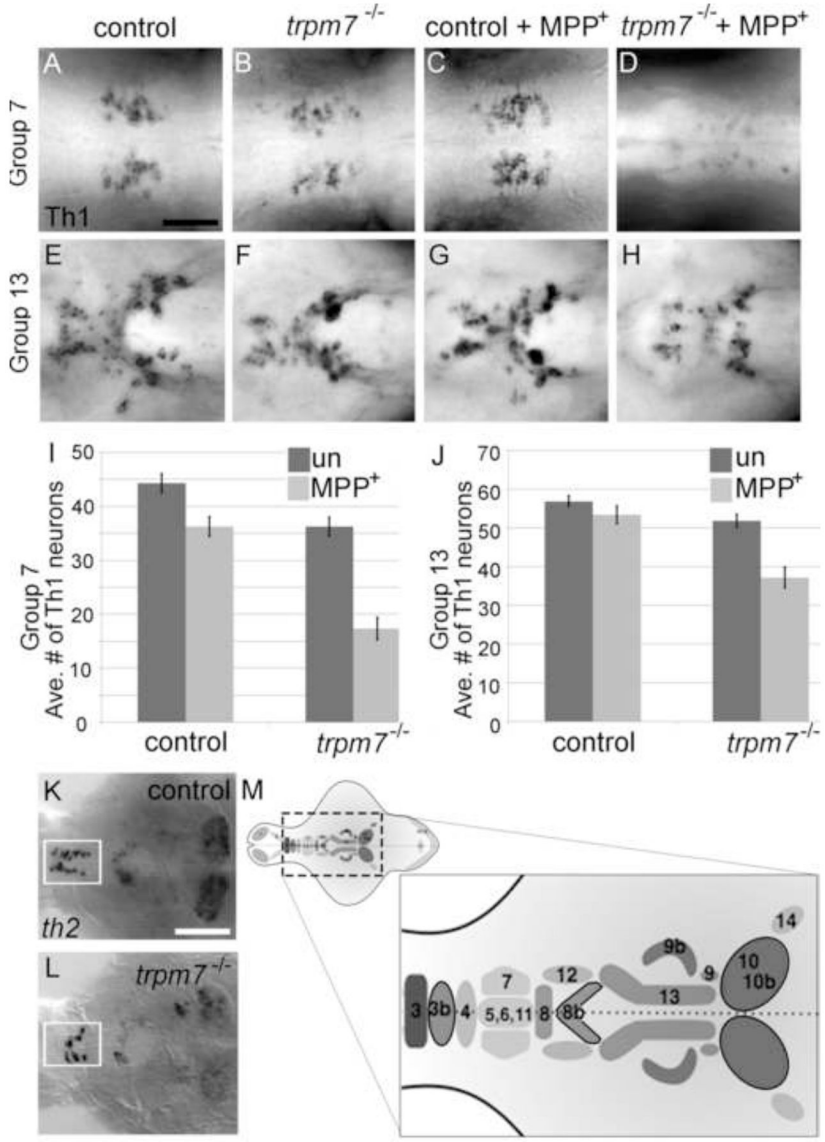

Figure 4. *trpm7* mutants are sensitized to MPP$^+$

A–H) Dorsal views of 5-dpf larvae of the indicated genotype, treated with 500 μm MPP$^+$ or vehicle control as indicated. Individual panels show distinct groups of Th1 IR cells in the following brain regions: **A–D)** pretectal diencephalon (group 7); **E–H)** periventricular hypothalamus (group 13); and **I,J)** average numbers of Th1 IR-positive cells in each group (n=11). In the untreated samples, the number of Th1 IR cells was significantly lower in mutants than controls in group 7 (control 44, mutant 36; Two way ANOVA with Bonferroni post-hoc test, $p < 0.001$). After MPP$^+$ treatment the difference was greater; this interaction of genotype and MPP$^+$ treatment was significant ($p < 0.001$). In group 13, (control 56, mutant 51) there was not a significant difference in the number of Th1 IR cells between untreated controls and untreated mutants however the interaction between genotype and MPP$^+$ treatment was significant ($p < 0.02$) (group 13: control + vehicle vs. control + MPP$^+$, $p > 0.05$; mutant + vehicle vs. mutant + MPP$^+$: $p < 0.001$). In both groups, MPP$^+$ treatment effected a larger reduction in the number of Th1 IR cells in mutants than in controls (group 7, control + MPP$^+$ 39, mutant + MPP$^+$ 17; group 13, control + MPP$^+$ 53, mutant + MPP$^+$ 37). In group 7 the effect of MPP$^+$ in mutants was almost three times larger than in controls,

and in group 13 it was over four times larger. **K,L)** Dorsal views of dissected brains from **K)** control or **L)** *trpm7* mutant larvae, processed to reveal *th2* mRNA. The pre-optic area (group 3b) is outlined in white. (*th2*-positive cells: control: 14, n=9; mutant: 7, n=12; $p < 0.001$). Scale bar in B=50 μm. Scale bar in L=100 μm. **M)** Schematic illustrating the numbering scheme of Th1 and *th2* positive (outlined in black) neuron clusters where darkness indicates more ventral groups (1 olfactory bulb; 2 subpallium; 3–4 preoptic area; 5,6,11 diencephalon; 7 pretectum; 8 anterior paraventricular organ; 9 interior paraventricular organ; 10 posterior paraventricular organ; 12 posterior tuberal nucleus; 13 hypothalamus; 14 locus coeruleus; 15–16 medulla oblongata; 17 area postrema; see Table S1 for additional details) (modified from (Sallinen et al., 2009).

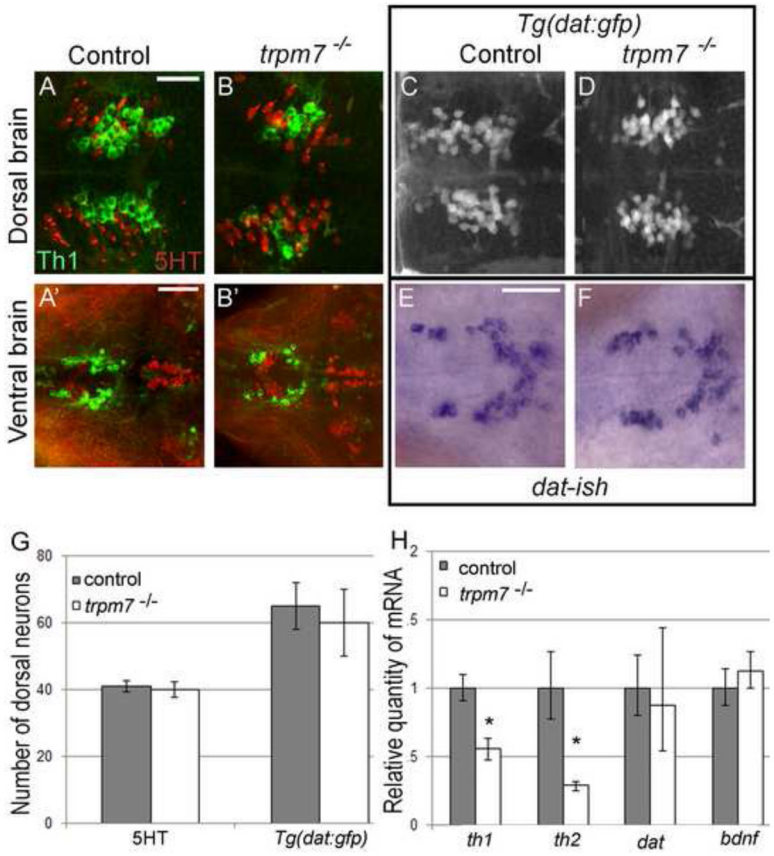

Figure 5. Numbers of serotonergic neurons and neurons expressing *dat* are normal in *trpm7* mutants A,B; A′,B′)

Dorsal views of the **A,B)** pre-tectum (Th1 group 7) and **A′,B′)** hypothalamus (Th1 group 13) in 5 dpf control and *trpm7* mutant larvae, as indicated, processed to reveal anti-5HT (red) and anti-Th1 (green) immunoreactivity (IR). Th1 IR cells were reduced in mutants (quantified in Fig. 4), 5HT IR cells were normal in number (below). Scale bar in A= 30 μm and applies to A-D; scale bar in A′= 50 μm and applies to A′–B′ and E, F. **C,D)** Dorsal views of 5 dpf *Tg(dat:gfp)* larvae focused on the pretectum (group 7). GFP-expressing neurons were equally abundant in *trpm7* mutants and controls (see panel G). **E,F)** Ventral view of hypothalamus (group 13) in embryos of the indicated genotype processed to reveal *dat* expression by *in situ* hybridization. **G)** Bar chart indicating numbers of 5HT IR and GFP-expressing neurons within the pretectum (group 7) of *trpm7* mutants (or *trpm7* mutant; *Tg(dat:gfp)* transgenic) and controls. Number of neurons was not significantly different between the genotypes. (With anti-Hu at 5 dpf tails of control larvae had 32 ± 0.4 dorsal root ganglia neurons while mutant larvae had 31 ± 0.5, where ± denotes SEM). **H)** qRT-PCR analysis of mRNA levels of *th1*, *th2*, *dat*, and *bdnf*. Asterisks indicate significant difference; * $p < 0.001$. Error bars represent SEM.

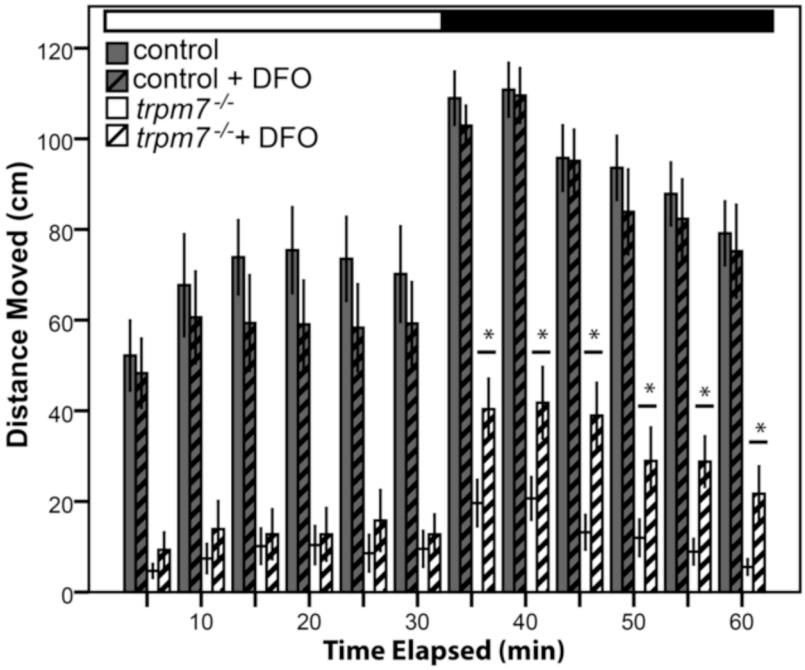

Figure 6. DFO partially rescues hypomotility of *trpm7* mutants

DFO treatment increased spontaneous motility of 5-dpf, *trpm7*^{b508} mutant larvae. Automated analysis of motility was carried out as in Fig. 2. For each experiment, half of a single clutch of larvae from *trpm7* heterozygous adults was treated with 50 μM DFO from 2–5 dpf. Motility of control larvae was unaffected by DFO treatment (Student's t-test, $p > 0.4$). Motility of the *trpm7* mutant was significantly increased by treatment with DFO in darkness (Student's t-test, $p < 0.05$). Each group tested consisted of 23–24 animals. Error bars represent SEM. Asterisks, significantly different values.

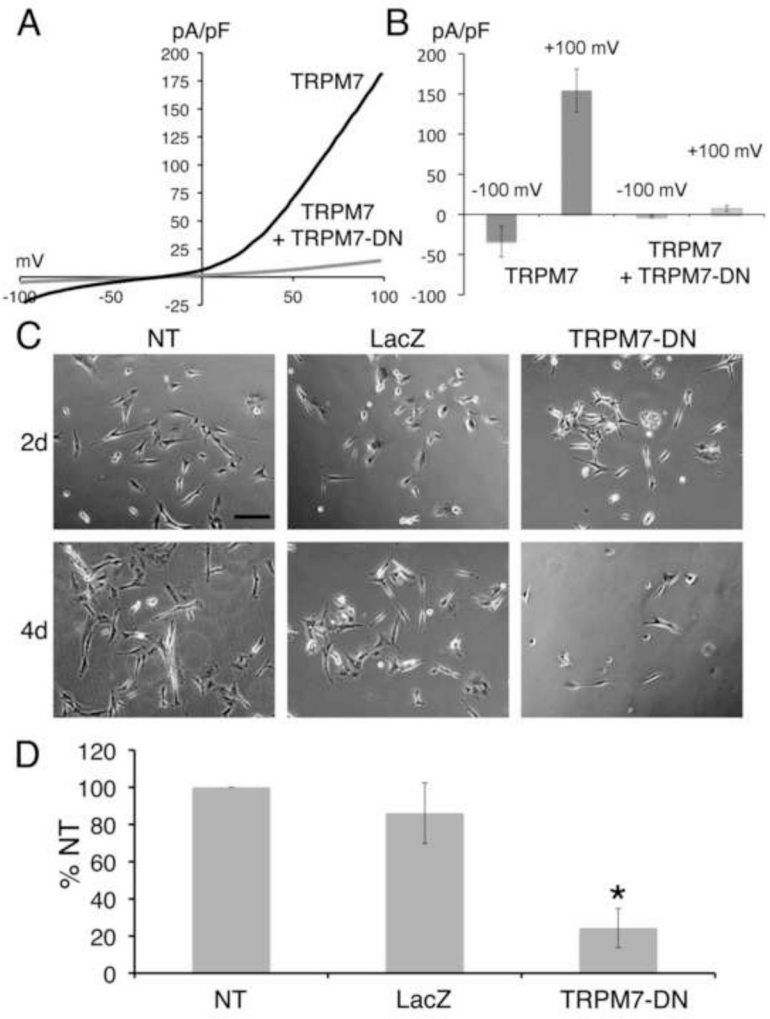

Figure 7. Expression of TRPM7 dominant-negative (TRPM7-DN) suppresses differentiation by causing cell death

A) Representative traces show the current-voltage relationship in HEK-293 cells with expression of wild-type TRPM7 alone or with coexpression of wild-type TRPM7 and the TRPM7-E1047K pore mutant (TRPM7-DN). **B)** Co-expression of TRPM7-DN with wild-type TRPM7 in HEK-293 cells suppressed TRPM7 current densities at −120 mV and +100 mV. **C)** Representative phase-contrast images of SH-SY5Y cells treated with retinoic acid (RA), at 4 and 6 days after plating. Shown are non-transduced (NT) cells, cells transduced with LacZ for 2 and 4 days, and cells transduced with TRPM7-DN for 2 and 4 days. Scale bar = 200 μm. **D)** Cell viability of non-transduced (NT), LacZ expressing, and TRPM7-DN expressing SH-SY5Y cells treated with RA 6 days after plating and 3 days post-transduction. Viability of TRPM7-DN transduced and NT cells was significantly different (Student's t-test, p=0.006). Viability was expressed as percent of non-transduced (% NT) cells.